

Measurement of the Proton-Air Cross Section at $\sqrt{s} = 57$ TeV with the Pierre Auger Observatory

P. Abreu,¹ M. Aglietta,² E. J. Ahn,³ I. F. M. Albuquerque,⁴ D. Allard,⁵ I. Allekotte,⁶ J. Allen,⁷ P. Allison,⁸ A. Almeda,^{9,10} J. Alvarez Castillo,¹¹ J. Alvarez-Muñiz,¹² M. Ambrosio,¹³ A. Aminaei,¹⁴ L. Anchordoqui,¹⁵ S. Andringa,¹ T. Antičić,¹⁶ C. Aramo,¹³ E. Arganda,^{17,18} F. Arqueros,¹⁸ H. Asorey,⁶ P. Assis,¹ J. Aublin,¹⁹ M. Ave,²⁰ M. Avenier,²¹ G. Avila,²² T. Bäcker,²³ M. Balzer,²⁴ K. B. Barber,²⁵ A. F. Barbosa,²⁶ R. Bardenet,²⁷ S. L. C. Barroso,²⁸ B. Baughman,⁸ J. Bäuml,²⁹ J. J. Beatty,⁸ B. R. Becker,³⁰ K. H. Becker,³¹ A. Bellétoile,³² J. A. Bellido,²⁵ S. BenZvi,³³ C. Berat,²¹ X. Bertou,⁶ P. L. Biermann,³⁴ P. Billoir,¹⁹ F. Blanco,¹⁸ M. Blanco,³⁵ C. Bleve,³¹ H. Blümer,^{20,29} M. Boháčová,³⁶ D. Boncioli,³⁷ C. Bonifazi,^{38,19} R. Bonino,² N. Borodai,³⁹ J. Brack,⁴⁰ P. Brogueira,¹ W. C. Brown,⁴¹ R. Bruijn,⁴² P. Buchholz,²³ A. Bueno,⁴³ R. E. Burton,⁴⁴ K. S. Caballero-Mora,⁴⁵ L. Caramete,³⁴ R. Caruso,⁴⁶ A. Castellina,² O. Catalano,⁴⁷ G. Cataldi,⁴⁸ L. Cazon,¹ R. Cester,⁴⁹ J. Chauvin,²¹ S. H. Cheng,⁴⁵ A. Chiavassa,² J. A. Chinellato,⁵⁰ J. Chirinos Diaz,⁵¹ J. Chudoba,³⁶ R. W. Clay,²⁵ M. R. Coluccia,⁴⁸ R. Conceição,¹ F. Contreras,⁵² H. Cook,⁴² M. J. Cooper,²⁵ J. Coppens,^{14,53} A. Cordier,²⁷ S. Coutu,⁴⁵ C. E. Covault,⁴⁴ A. Creusot,^{5,54} A. Criss,⁴⁵ J. Cronin,⁵⁵ A. Curutiu,³⁴ S. Dagoret-Campagne,²⁷ R. Dallier,³² S. Dasso,^{56,57} K. Daumiller,²⁹ B. R. Dawson,²⁵ R. M. de Almeida,⁵⁸ M. De Domenico,⁴⁶ C. De Donato,¹¹ S. J. de Jong,^{14,53} G. De La Vega,⁵⁹ W. J. M. de Mello Junior,⁵⁰ J. R. T. de Mello Neto,³⁸ I. De Mitri,⁴⁸ V. de Souza,⁶⁰ K. D. de Vries,⁶¹ G. Decerprit,⁵ L. del Peral,³⁵ M. del Río,^{37,52} O. Deligny,⁶² H. Dembinski,²⁰ N. Dhital,⁵¹ C. Di Giulio,⁶³ M. L. Díaz Castro,⁶⁴ P. N. Diep,⁶⁵ C. Dobrigkeit,⁵⁰ W. Docters,⁶¹ J. C. D'Olivo,¹¹ P. N. Dong,^{65,62} A. Dorofeev,⁴⁰ J. C. dos Anjos,²⁶ M. T. Dova,¹⁷ D. D'Urso,¹³ I. Dutan,³⁴ J. Ebr,³⁶ R. Engel,²⁹ M. Erdmann,⁶⁶ C. O. Escobar,⁵⁰ J. Espadanal,¹ A. Etchegoyen,^{10,9} P. Facal San Luis,⁵⁵ I. Fajardo Tapia,¹¹ H. Falcke,^{14,67} G. Farrar,⁷ A. C. Fauth,⁵⁰ N. Fazzini,³ A. P. Ferguson,⁴⁴ A. Ferrero,¹⁰ B. Fick,⁵¹ A. Filevich,¹⁰ A. Filipčić,^{68,54} S. Fliescher,⁶⁶ C. E. Fracchiolla,⁴⁰ E. D. Fraenkel,⁶¹ U. Fröhlich,²³ B. Fuchs,²⁶ R. Gaior,¹⁹ R. F. Gamarra,¹⁰ S. Gambetta,⁶⁹ B. García,⁵⁹ D. Garcia-Gamez,²⁷ D. Garcia-Pinto,¹⁸ A. Gascon,⁴³ H. Gemmeke,²⁴ K. Gesterling,³⁰ P. L. Ghia,^{19,2} U. Giaccari,⁴⁸ M. Giller,⁷⁰ H. Glass,³ M. S. Gold,³⁰ G. Golup,⁶ F. Gomez Albarracin,¹⁷ M. Gómez Berisso,⁶ P. Gonçalves,¹ D. Gonzalez,²⁰ J. G. Gonzalez,²⁰ B. Gookin,⁴⁰ D. Góra,^{20,39} A. Gorgi,² P. Gouffon,⁴ S. R. Gozzini,⁴² E. Grashorn,⁸ S. Grebe,^{14,53} N. Griffith,⁸ M. Grigat,⁶⁶ A. F. Grillo,⁷¹ Y. Guardincerri,⁵⁷ F. Guarino,¹³ G. P. Guedes,⁷² A. Guzman,¹¹ J. D. Hague,³⁰ P. Hansen,¹⁷ D. Harari,⁶ S. Harmsma,^{61,53} T. A. Harrison,²⁵ J. L. Harton,⁴⁰ A. Haungs,²⁹ T. Hebbeker,⁶⁶ D. Heck,²⁹ A. E. Herve,²⁵ C. Hojvat,³ N. Hollon,⁵⁵ V. C. Holmes,²⁵ P. Homola,³⁹ J. R. Hörandel,¹⁴ A. Horneffer,¹⁴ P. Horvath,⁷³ M. Hrabovský,^{73,36} T. Huege,²⁹ A. Insolia,⁴⁶ F. Ionita,⁵⁵ A. Italiano,⁴⁶ C. Jarne,¹⁷ S. Jiraskova,¹⁴ M. Josebachuili,¹⁰ K. Kadija,¹⁶ K. H. Kampert,³¹ P. Karhan,⁷⁴ P. Kasper,³ B. Kégl,²⁷ B. Keilhauer,²⁹ A. Keivani,⁷⁵ J. L. Kelley,¹⁴ E. Kemp,⁵⁰ R. M. Kieckhafer,⁵¹ H. O. Klages,²⁹ M. Kleifges,²⁴ J. Kleinfeller,²⁹ J. Knapp,⁴² D.-H. Koang,²¹ K. Kotera,⁵⁵ N. Krohm,³¹ O. Krömer,²⁴ D. Krupke-Hansen,³¹ F. Kuehn,³ D. Kuempel,³¹ J. K. Kulbartz,⁷⁶ N. Kunka,²⁴ G. La Rosa,⁴⁷ C. Lachaud,⁵ R. Lauer,³⁰ P. Lautridou,³² S. Le Coz,²¹ M. S. A. B. Leão,⁷⁷ D. Lebrun,²¹ P. Lebrun,³ M. A. Leigui de Oliveira,⁷⁷ A. Lemiere,⁶² A. Letessier-Selvon,¹⁹ I. Lhenry-Yvon,⁶² K. Link,²⁰ R. López,⁷⁸ A. Lopez Agüera,¹² K. Louedec,^{21,27} J. Lozano Bahilo,⁴³ L. Lu,⁴² A. Lucero,^{10,2} M. Ludwig,²⁰ H. Lyberis,⁶² C. Macolino,¹⁹ S. Maldera,² D. Mandat,³⁶ P. Mantsch,³ A. G. Mariuzzi,¹⁷ J. Marin,^{52,2} V. Marin,³² I. C. Maris,¹⁹ H. R. Marquez Falcon,⁷⁹ G. Marsella,⁸⁰ D. Martello,⁴⁸ L. Martin,³² H. Martinez,⁸¹ O. Martínez Bravo,⁷⁸ H. J. Mathes,²⁹ J. Matthews,^{75,82} J. A. J. Matthews,³⁰ G. Matthiae,³⁷ D. Maurizio,⁴⁹ P. O. Mazur,³ G. Medina-Tanco,¹¹ M. Melissas,²⁰ D. Melo,^{10,49} E. Menichetti,⁴⁹ A. Menshikov,²⁴ P. Mertsch,⁸³ C. Meurer,⁶⁶ S. Mićanović,¹⁶ M. I. Micheletti,⁸⁴ W. Miller,³⁰ L. Miramonti,⁸⁵ L. Molina-Bueno,⁴³ S. Mollerach,⁶ M. Monasor,⁵⁵ D. Monnier Ragainie,²⁷ F. Montanet,²¹ B. Morales,¹¹ C. Morello,² E. Moreno,⁷⁸ J. C. Moreno,¹⁷ C. Morris,⁸ M. Mostafá,⁴⁰ C. A. Moura,^{77,13} S. Mueller,²⁹ M. A. Muller,⁵⁰ G. Müller,⁶⁶ M. Münchmeyer,¹⁹ R. Mussa,⁴⁹ G. Navarra,² J. L. Navarro,⁴³ S. Navas,⁴³ P. Necasal,³⁶ L. Nellen,¹¹ A. Nelles,^{14,53} J. Neuser,³¹ P. T. Nhung,⁶⁵ L. Niemietz,³¹ N. Nierstenhoefer,³¹ D. Nitz,⁵¹ D. Nosek,⁷⁴ L. Nožka,³⁶ M. Nyklicek,³⁶ J. Oehlschläger,²⁹ A. Olinto,⁵⁵ V. M. Olmos-Gilbaja,¹² M. Ortiz,¹⁸ N. Pacheco,³⁵ D. Pakk Selmi-Dei,⁵⁰ M. Palatka,³⁶ J. Pallotta,⁸⁶ N. Palmieri,²⁰ G. Parente,¹² E. Parizot,⁵ A. Parra,¹² R. D. Parsons,⁴² S. Pastor,⁸⁷ T. Paul,⁸⁸ M. Pech,³⁶ J. Pečala,³⁹ R. Pelayo,^{78,12} I. M. Pepe,⁸⁹ L. Perrone,⁸⁰ R. Pesce,⁶⁹ E. Petermann,⁹⁰ S. Petrera,⁶³ P. Petrinca,³⁷ A. Petrolini,⁶⁹ Y. Petrov,⁴⁰ J. Petrovic,⁵³ C. Pfendner,³³ N. Phan,³⁰ R. Piegai,⁵⁷ T. Pierog,²⁹ P. Pieroni,⁵⁷ M. Pimenta,¹ V. Pirronello,⁴⁶ M. Platino,¹⁰ V. H. Ponce,⁶ M. Pontz,²³ P. Privitera,⁵⁵ M. Prouza,³⁶ E. J. Quel,⁸⁶ S. Querchfeld,³¹ J. Rautenberg,³¹ O. Ravel,³² D. Ravignani,¹⁰ B. Revenu,³² J. Ridky,³⁶ S. Riggi,^{12,46} M. Risse,²³ P. Ristori,⁸⁶ H. Rivera,⁸⁵ V. Rizi,⁶³ J. Roberts,⁷ C. Robledo,⁷⁸ W. Rodrigues de Carvalho,^{12,4} G. Rodriguez,¹² J. Rodriguez Martino,⁵² J. Rodriguez Rojo,⁵² I. Rodriguez-Cabo,¹²

M. D. Rodríguez-Frías,³⁵ G. Ros,³⁵ J. Rosado,¹⁸ T. Rossler,⁷³ M. Roth,²⁹ B. Rouillé-d'Orfeuille,⁵⁵ E. Roulet,⁶ A. C. Rovero,⁵⁶ C. Rühle,²⁴ F. Salamida,^{62,63} H. Salazar,⁷⁸ F. Salesa Greus,⁴⁰ G. Salina,³⁷ F. Sánchez,¹⁰ C. E. Santo,¹ E. Santos,¹ E. M. Santos,³⁸ F. Sarazin,⁹¹ B. Sarkar,³¹ S. Sarkar,⁸³ R. Sato,⁵² N. Scharf,⁶⁶ V. Scherini,⁸⁵ H. Schieler,²⁹ P. Schiffer,^{76,66} A. Schmidt,²⁴ O. Scholten,⁶¹ H. Schoorlemmer,^{14,53} J. Schovancova,³⁶ P. Schovánek,³⁶ F. Schröder,²⁹ S. Schulte,⁶⁶ D. Schuster,⁹¹ S. J. Sciutto,¹⁷ M. Scuderi,⁴⁶ A. Segreto,⁴⁷ M. Settimo,²³ A. Shadkam,⁷⁵ R. C. Shellard,^{26,64} I. Sidelnik,¹⁰ G. Sigl,⁷⁶ H. H. Silva Lopez,¹¹ A. Śmiałkowski,⁷⁰ R. Šmída,^{29,36} G. R. Snow,⁹⁰ P. Sommers,⁴⁵ J. Sorokin,²⁵ H. Spinka,^{92,3} R. Squartini,⁵² S. Stanic,⁵⁴ J. Stapleton,⁸ J. Stasielak,³⁹ M. Stephan,⁶⁶ A. Stutz,²¹ F. Suarez,¹⁰ T. Suomijärvi,⁶² A. D. Supanitsky,^{56,11} T. Šušá,¹⁶ M. S. Sutherland,^{75,8} J. Swain,⁸⁸ Z. Szadkowski,⁷⁰ M. Szuba,²⁹ A. Tamashiro,⁵⁶ A. Tapia,¹⁰ M. Tartare,²¹ O. Taşcau,³¹ C. G. Tavera Ruiz,¹¹ R. Tcaciuc,²³ D. Tegolo,^{46,93} N. T. Thao,⁶⁵ D. Thomas,⁴⁰ J. Tiffenberg,⁵⁷ C. Timmermans,^{53,14} D. K. Tiwari,⁷⁹ W. Tkaczyk,⁷⁰ C. J. Todero Peixoto,^{60,77} B. Tomé,¹ A. Tonachini,⁴⁹ P. Travnicek,³⁶ D. B. Tridapalli,⁴ G. Tristram,⁵ E. Trovato,⁴⁶ M. Tueros,^{12,57} R. Ulrich,^{29,45} M. Unger,²⁹ M. Urban,²⁷ J. F. Valdés Galicia,¹¹ I. Valiño,¹² L. Valore,¹³ A. M. van den Berg,⁶¹ E. Varela,⁷⁸ B. Vargas Cárdenas,¹¹ J. R. Vázquez,¹⁸ R. A. Vázquez,¹² D. Veberič,^{54,68} V. Verzi,³⁷ J. Vicha,³⁶ M. Videla,⁵⁹ L. Villaseñor,⁷⁹ H. Wahlberg,¹⁷ P. Wahrlich,²⁵ O. Wainberg,^{10,9} D. Walz,⁶⁶ D. Warner,⁴⁰ A. A. Watson,⁴² M. Weber,²⁴ K. Weidenhaupt,⁶⁶ A. Weindl,²⁹ S. Westerhoff,³³ B. J. Whelan,²⁵ G. Wieczorek,⁷⁰ L. Wiencke,⁹¹ B. Wilczyńska,³⁹ H. Wilczyński,³⁹ M. Will,²⁹ C. Williams,⁵⁵ T. Winchen,⁶⁶ M. G. Winnick,²⁵ M. Wommer,²⁹ B. Wundheiler,¹⁰ T. Yamamoto,⁵⁵ T. Yapici,⁵¹ P. Younk,^{23,94} G. Yuan,⁷⁵ A. Yushkov,^{12,13} B. Zamorano,⁴³ E. Zas,¹² D. Zavrtanik,^{54,68} M. Zavrtanik,^{68,54} I. Zaw,⁷ A. Zepeda,⁸¹ Y. Zhu,²⁴ M. Zimbres Silva,^{31,50} and M. Ziolkowski²³

(The Pierre Auger Collaboration)

¹LIP and Instituto Superior Técnico, Technical University of Lisbon, Portugal

²Istituto di Fisica dello Spazio Interplanetario (INAF), Università di Torino and Sezione INFN, Torino, Italy

³Fermilab, Batavia, Illinois, USA

⁴Universidade de São Paulo, Instituto de Física, São Paulo, SP, Brazil

⁵Laboratoire AstroParticule et Cosmologie (APC), Université Paris 7, CNRS-IN2P3, Paris, France

⁶Centro Atómico Bariloche and Instituto Balseiro (CNEA-UNCuyo-CONICET), San Carlos de Bariloche, Argentina

⁷New York University, New York, New York, USA

⁸Ohio State University, Columbus, Ohio, USA

⁹Universidad Tecnológica Nacional-Facultad Regional Buenos Aires, Buenos Aires, Argentina

¹⁰Instituto de Tecnologías en Detección y Astropartículas (CNEA, CONICET, UNSAM), Buenos Aires, Argentina

¹¹Universidad Nacional Autónoma de México, México, D.F., México

¹²Universidad de Santiago de Compostela, Spain

¹³Università di Napoli "Federico II" and Sezione INFN, Napoli, Italy

¹⁴IMAPP, Radboud University Nijmegen, Netherlands

¹⁵University of Wisconsin, Milwaukee, Wisconsin, USA

¹⁶Rudjer Bošković Institute, 10000 Zagreb, Croatia

¹⁷IFLP, Universidad Nacional de La Plata and CONICET, La Plata, Argentina

¹⁸Universidad Complutense de Madrid, Madrid, Spain

¹⁹Laboratoire de Physique Nucléaire et de Hautes Energies (LPNHE), Universités Paris 6 et Paris 7, CNRS-IN2P3, Paris, France

²⁰Karlsruhe Institute of Technology-Campus South-Institut für Experimentelle Kernphysik (IEKP), Karlsruhe, Germany

²¹Laboratoire de Physique Subatomique et de Cosmologie (LPSC), Université Joseph Fourier, INPG, CNRS-IN2P3, Grenoble, France

²²Observatorio Pierre Auger and Comisión Nacional de Energía Atómica, Malargüe, Argentina

²³Universität Siegen, Siegen, Germany

²⁴Karlsruhe Institute of Technology-Campus North-Institut für Prozessdatenverarbeitung und Elektronik, Karlsruhe, Germany

²⁵University of Adelaide, Adelaide, S.A., Australia

²⁶Centro Brasileiro de Pesquisas Físicas, Rio de Janeiro, RJ, Brazil

²⁷Laboratoire de l'Accélérateur Linéaire (LAL), Université Paris 11, CNRS-IN2P3, Orsay, France

²⁸Universidade Estadual do Sudoeste da Bahia, Vitória da Conquista, BA, Brazil

²⁹Karlsruhe Institute of Technology-Campus North-Institut für Kernphysik, Karlsruhe, Germany

³⁰University of New Mexico, Albuquerque, New Mexico, USA

³¹Bergische Universität Wuppertal, Wuppertal, Germany

³²SUBATECH, École des Mines de Nantes, CNRS-IN2P3, Université de Nantes, Nantes, France

³³University of Wisconsin, Madison, Wisconsin, USA

³⁴Max-Planck-Institut für Radioastronomie, Bonn, Germany

³⁵Universidad de Alcalá, Alcalá de Henares (Madrid), Spain

³⁶Institute of Physics of the Academy of Sciences of the Czech Republic, Prague, Czech Republic

- ³⁷Università di Roma II “Tor Vergata” and Sezione INFN, Roma, Italy
- ³⁸Universidade Federal do Rio de Janeiro, Instituto de Física, Rio de Janeiro, RJ, Brazil
- ³⁹Institute of Nuclear Physics PAN, Krakow, Poland
- ⁴⁰Colorado State University, Fort Collins, Colorado, USA
- ⁴¹Colorado State University, Pueblo, Colorado, USA
- ⁴²School of Physics and Astronomy, University of Leeds, United Kingdom
- ⁴³Universidad de Granada and C.A.F.P.E., Granada, Spain
- ⁴⁴Case Western Reserve University, Cleveland, Ohio, USA
- ⁴⁵Pennsylvania State University, University Park, Pennsylvania, USA
- ⁴⁶Università di Catania and Sezione INFN, Catania, Italy
- ⁴⁷Istituto di Astrofisica Spaziale e Fisica Cosmica di Palermo (INAF), Palermo, Italy
- ⁴⁸Dipartimento di Fisica dell’Università del Salento and Sezione INFN, Lecce, Italy
- ⁴⁹Università di Torino and Sezione INFN, Torino, Italy
- ⁵⁰Universidade Estadual de Campinas, IFGW, Campinas, SP, Brazil
- ⁵¹Michigan Technological University, Houghton, Michigan, USA
- ⁵²Observatorio Pierre Auger, Malargüe, Argentina
- ⁵³Nikhef, Science Park, Amsterdam, Netherlands
- ⁵⁴Laboratory for Astroparticle Physics, University of Nova Gorica, Slovenia
- ⁵⁵University of Chicago, Enrico Fermi Institute, Chicago, Illinois, USA
- ⁵⁶Instituto de Astronomía y Física del Espacio (CONICET-UBA), Buenos Aires, Argentina
- ⁵⁷Departamento de Física, FCEyN, Universidad de Buenos Aires y CONICET, Argentina
- ⁵⁸Universidade Federal Fluminense, EEIMVR, Volta Redonda, RJ, Brazil
- ⁵⁹National Technological University, Faculty Mendoza (CONICET/CNEA), Mendoza, Argentina
- ⁶⁰Universidade de São Paulo, Instituto de Física, São Carlos, SP, Brazil
- ⁶¹Kernfysisch Versneller Instituut, University of Groningen, Groningen, Netherlands
- ⁶²Institut de Physique Nucléaire d’Orsay (IPNO), Université Paris 11, CNRS-IN2P3, Orsay, France
- ⁶³Università dell’Aquila and INFN, L’Aquila, Italy
- ⁶⁴Pontifícia Universidade Católica, Rio de Janeiro, RJ, Brazil
- ⁶⁵Institute for Nuclear Science and Technology (INST), Hanoi, Vietnam
- ⁶⁶RWTH Aachen University, III. Physikalisches Institut A, Aachen, Germany
- ⁶⁷ASTRON, Dwingeloo, Netherlands
- ⁶⁸J. Stefan Institute, Ljubljana, Slovenia
- ⁶⁹Dipartimento di Fisica dell’Università and INFN, Genova, Italy
- ⁷⁰University of Łódź, Łódź, Poland
- ⁷¹INFN, Laboratori Nazionali del Gran Sasso, Assergi (L’Aquila), Italy
- ⁷²Universidade Estadual de Feira de Santana, Brazil
- ⁷³Palacky University, RCPTM, Olomouc, Czech Republic
- ⁷⁴Charles University, Faculty of Mathematics and Physics, Institute of Particle and Nuclear Physics, Prague, Czech Republic
- ⁷⁵Louisiana State University, Baton Rouge, Louisiana, USA
- ⁷⁶Universität Hamburg, Hamburg, Germany
- ⁷⁷Universidade Federal do ABC, Santo André, SP, Brazil
- ⁷⁸Benemérita Universidad Autónoma de Puebla, Puebla, Mexico
- ⁷⁹Universidad Michoacana de San Nicolas de Hidalgo, Morelia, Michoacan, Mexico
- ⁸⁰Dipartimento di Ingegneria dell’Innovazione dell’Università del Salento and Sezione INFN, Lecce, Italy
- ⁸¹Centro de Investigación y de Estudios Avanzados del IPN (CINVESTAV), México, D.F., Mexico
- ⁸²Southern University, Baton Rouge, Louisiana, USA
- ⁸³Rudolf Peierls Centre for Theoretical Physics, University of Oxford, Oxford, United Kingdom
- ⁸⁴Instituto de Física de Rosario (IFIR)-CONICET/U.N.R.
and Facultad de Ciencias Bioquímicas y Farmacéuticas U.N.R., Rosario, Argentina
- ⁸⁵Università di Milano and Sezione INFN, Milan, Italy
- ⁸⁶Centro de Investigaciones en Láseres y Aplicaciones, CITEFA and CONICET, Argentina
- ⁸⁷Instituto de Física Corpuscular, CSIC-Universitat de València, Valencia, Spain
- ⁸⁸Northeastern University, Boston, Massachusetts, USA
- ⁸⁹Universidade Federal da Bahia, Salvador, BA, Brazil
- ⁹⁰University of Nebraska, Lincoln, Nebraska, USA
- ⁹¹Colorado School of Mines, Golden, Colorado, USA
- ⁹²Argonne National Laboratory, Argonne, Illinois, USA
- ⁹³Università di Palermo and Sezione INFN, Catania, Italy
- ⁹⁴Los Alamos National Laboratory, Los Alamos, New Mexico, USA

(Received 2 September 2011; published 10 August 2012)

We report a measurement of the proton-air cross section for particle production at the center-of-mass energy per nucleon of 57 TeV. This is derived from the distribution of the depths of shower maxima observed with the Pierre Auger Observatory: systematic uncertainties are studied in detail. Analyzing the tail of the distribution of the shower maxima, a proton-air cross section of $[505 \pm 22(\text{stat})_{-36}^{+28}(\text{syst})]$ mb is found.

DOI: [10.1103/PhysRevLett.109.062002](https://doi.org/10.1103/PhysRevLett.109.062002)

PACS numbers: 13.85.Tp, 96.50.sd

Introduction.—We present an analysis of the proton-air cross section based on measurements made at the Pierre Auger Observatory [1]. For this purpose, we analyze the shape of the distribution of the largest values of the depth of shower maximum, X_{max} , the position at which an air shower deposits the maximum energy per unit of mass of atmosphere traversed. The *tail* of the X_{max} distribution is sensitive to the proton-air cross section, a fact exploited in the pioneering work of the Fly’s Eye Collaboration [2]. To obtain accurate measurements of X_{max} , timing data from the fluorescence telescopes are combined with that from the surface detector array for a precise hybrid reconstruction of the geometry of events [3].

We place particular emphasis on studying systematic uncertainties in the cross-section analysis. The unknown mass composition of cosmic rays [4] is identified to be the major source of systematic uncertainty and accordingly the analysis has been optimized to minimize the impact of particles other than protons in the primary beam. This begins with restricting the analysis to the energy interval 10^{18} to $10^{18.5}$ eV, where the shape of the X_{max} distribution is compatible with there being a substantial fraction of protons; also there are a large number of events recorded in this energy range. The corresponding average center-of-mass energy of a proton interacting with a nucleon is 57 TeV, significantly above the reach of the Large Hadron Collider.

Analysis approach.—The proton-air cross section is derived in a two-step process. First, we measure an air shower observable with high sensitivity to the cross section. Second, we convert this measurement to a value of the proton-air cross section for particle production (cf. [5]). This is the cross section that accounts for all interactions which produce particles and thus contribute to the air-shower development; it implicitly also includes diffractive interactions. As the primary observable, we define Λ_η via the exponential shape of the tail of the X_{max} distribution, $dN/dX_{\text{max}} \propto \exp(-X_{\text{max}}/\Lambda_\eta)$, where η denotes the fraction of most deeply penetrating air showers used. Considering only these events enhances the contribution of protons in the sample, since the depth at which proton-induced showers maximize is deeper in the atmosphere than for showers from heavier nuclei. Thus, η is a key parameter: a small value enhances the proton fraction, but reduces the number of events available for the analysis. We have chosen $\eta = 0.2$ so that, for helium-fractions up to 25%, biases introduced by the possible presence of helium and heavier nuclei do not exceed the level of the statistical uncertainty. This was chosen after a Monte Carlo study that

probed, for different values of η , the sensitivity of the analysis to the mass composition.

The measurement of Λ_η We use events collected between 1 December 2004 and 20 September 2010. The atmospheric and event-quality cuts applied are identical to those used for the analysis of $\langle X_{\text{max}} \rangle$ and $\text{rms}(X_{\text{max}})$ [6] yielding 11 628 high-quality events. The X_{max} distribution of these data is affected by the known geometrical acceptance of the fluorescence telescopes as well as by limitations related to atmospheric light transmission. We use the strategy developed for the measurement of $\langle X_{\text{max}} \rangle$ and $\text{rms}(X_{\text{max}})$ to extract a sample that has an unbiased X_{max} distribution: a fiducial volume selection, which requires event geometries that allow, for each individual shower, the complete observation of a defined slant depth range.

First, we derive the range of values of X_{max} that corresponds to the fraction $\eta = 0.2$ of the most deeply penetrating showers. For this we need an unbiased distribution of X_{max} over the entire depth range of observed values of X_{max} . To achieve this, we perform a fiducial event selection of the slant depth range containing 99.8% of the observed X_{max} distribution, which corresponds to the range from 550 to 1004 g/cm². This reduces the data sample to 1635 events, providing an unbiased X_{max} distribution that is used to find the range of values of X_{max} corresponding to $\eta = 0.2$, identified to extend from 768 to 1004 g/cm².

Second, we select those events from the original 11 628 that have geometries allowing the complete observation of values of X_{max} from 768 to 1004 g/cm², the tail of the unbiased distribution. This fiducial cut maximizes the statistics of an unbiased X_{max} distribution in the range of interest. In total, 3082 events pass the fiducial volume cuts, of which 783 events have their X_{max} in the selected range and thus contribute directly to the measurement of Λ_η . In Fig. 1 we show the 3082 selected events and the result of an unbinned maximum likelihood fit of an exponential function over the range 768 to 1004 g/cm². Values of Λ_η have been recalculated for subsamples of the full data set selected according to zenith angle, shower-to-telescope distance, and energy: the different values obtained for Λ_η are consistent with statistical fluctuations. The reanalyses of the data for changes of fiducial event selection, modified values of η , and for different ranges of atmospheric depths yield changes of Λ_η that are distributed around zero with a root-mean-square of 1.6 g/cm². We use this root-mean-square as an estimate of the systematic uncertainties associated with the measurement. This yields

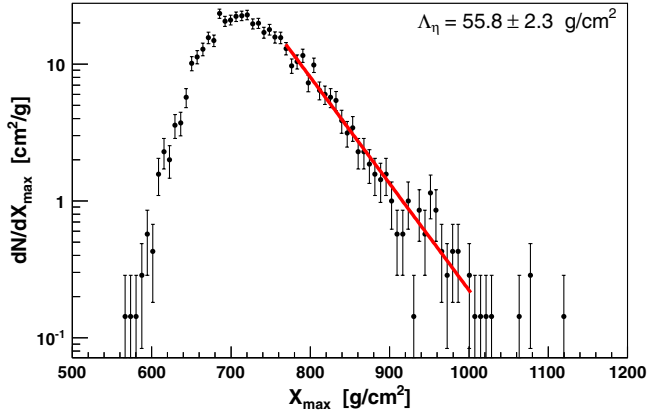


FIG. 1 (color online). Unbinned likelihood fit to obtain Λ_η (thick line). The X_{\max} distribution is unbiased by the fiducial geometry selection applied in the range of the fit.

$$\Lambda_\eta = 55.8 \pm 2.3(\text{stat}) \pm 1.6(\text{syst}) \text{ g/cm}^2, \quad (1)$$

with the average energy of these events being $10^{18.24 \pm 0.005(\text{stat})}$ eV. The differential energy distribution for these events follows a power law with index -1.9 . The average energy corresponds to a center-of-mass energy of $\sqrt{s} = 57 \pm 0.3(\text{stat})$ TeV in proton-proton collisions.

Determination of the cross section.—The determination of the proton-air cross section for particle production requires the use of air-shower simulations, which inherently introduces some dependence on model assumptions. We emulate the measurement of Λ_η with Monte Carlo simulations to derive predictions of the slope, Λ_η^{MC} . It is known from previous work that the values of Λ_η^{MC} are directly linked to the hadronic cross sections used in the simulations [2]. Accordingly we can explore the effect of changing cross sections empirically by multiplying all hadronic cross sections input to the simulations by an energy-dependent factor [7]

$$f(E, f_{19}) = 1 + (f_{19} - 1) \frac{\lg(E/10^{15} \text{ eV})}{\lg(10^{19} \text{ eV}/10^{15} \text{ eV})}, \quad (2)$$

where E denotes the shower energy and f_{19} is the factor by which the cross section is rescaled at 10^{19} eV. This factor is unity below 10^{15} eV, reflecting the fact that measurements of the cross section at the Tevatron were used to tune the interaction models. This technique of modifying the original predictions of the cross sections during the simulation process assures a smooth transition from accelerator data up to the energies of our analysis.

For each hadronic interaction model, the value of f_{19} is obtained that reproduces the measured value of Λ_η . The modified cross section is then deduced by multiplying the original cross section used in the model by the factor $f(E, f_{19})$ of Eq. (2) using $E = 10^{18.24}$ eV. For the conversion of Λ_η into cross section, we have used the four

high-energy hadronic interaction models commonly adopted for air-shower simulations: QGSJET01 [8], QGSJETII.3 [9], SIBYLL 2.1 [10], and EPOS1.99 [11]. While in general no model gives a completely accurate representation of cosmic-ray data in all respects, these have been found to give reasonably good descriptions of many of the main features. It has been shown [12] that the differences between the models used in the analysis are typically bigger than the variations obtained within one model by parameter variation. Therefore we use the model differences for estimating the systematic model dependence.

The proton-air cross sections for particle production derived for QGSJET01, QGSJETII, SIBYLL, and EPOS are 523.7, 502.9, 496.7, and 497.7 mb, respectively, with the statistical uncertainty for each of these values being 22 mb. The difference of these cross sections from the original model predictions are $<5\%$, with the exception of the result obtained with the SIBYLL model, which is 12% smaller than the original SIBYLL prediction. We use the maximum deviations derived from using the four models, relative to the average result of 505 mb, to estimate a systematic uncertainty of $(-8, +19)$ mb related to the difficulties of modeling high-energy interactions. This procedure relies on the coverage of the underlying theoretical uncertainties by the available models. For example, diffraction, fragmentation, inelastic intermediate states, nuclear effects, QCD saturation, etc., are all described at different levels using different phenomenological, but self-consistent, approaches in these models. It is thus possible that the true range of the uncertainty for air-shower analyses is larger, but this cannot be estimated with these models. Furthermore, certain features of hadronic particle production, such as the multiplicity, elasticity, and pion-charge ratio, have an especially important impact on air-shower development [13,14]; of these we found that only the elasticity can have a relevant impact on Λ_η . The identified systematic uncertainty of $(-8, +19)$ mb induced by the modeling of hadronic interactions corresponds to the impact of modifying the elasticity within $\pm(10-25)\%$ in the models.

The selection of events with large values of X_{\max} also enhances the fraction of primary cosmic-ray interactions with smaller multiplicities and larger elasticities, which is, for example, characteristic for diffractive interactions. The value of Λ_η is thus more sensitive to the cross section of those interactions. The identified model dependence for the determination of $\sigma_{p\text{-air}}^{\text{prod}}$ is also caused by the compensation of this effect.

Also the choice of a logarithmic energy dependence for the rescaling factor in Eq. (2) may affect the resulting cross sections. However, since the required rescaling factors are small, this can only be a marginal effect.

The systematic uncertainty of 22% [15] in the absolute value of the energy scale leads to systematic uncertainties of 7 mb in the cross section and 6 TeV in the center-of-mass

TABLE I. Summary of the systematic uncertainties.

Description	Impact on $\sigma_{p\text{-air}}^{\text{prod}}$
Λ_η systematics	± 15 mb
Hadronic interaction models	$-8 + 19$ mb
Energy scale	± 7 mb
Conversion of Λ_η to $\sigma_{p\text{-air}}^{\text{prod}}$	± 7 mb
Photons, $<0.5\%$	$< + 10$ mb
Helium, 10%	-12 mb
Helium, 25%	-30 mb
Helium, 50%	-80 mb
Total (25% helium)	-36 mb, $+28$ mb

energy. Furthermore, the procedure to obtain $\sigma_{p\text{-air}}^{\text{prod}}$ from the measured Λ_η depends on additional parameters. By varying the energy distribution, energy and X_{max} resolution in the simulations, we find that related systematic changes of the value of $\sigma_{p\text{-air}}^{\text{prod}}$ are distributed with a root-mean-square of 7 mb around zero. We use the root-mean-square as estimate of the systematic uncertainties related to the conversion of Λ_η to $\sigma_{p\text{-air}}^{\text{prod}}$.

The presence of photons in the primary beam would bias the measurement. The average X_{max} of showers produced by photons at the energies of interest is about 50 g/cm² deeper in the atmosphere than that of protons. However, observational limits on the fraction of photons are $<0.5\%$ [16,17]. With simulations we find that the possible underestimation of the cross section if photons were present in the data sample at this level is less than 10 mb.

With the present limitations of observations, we cannot distinguish air showers produced by helium nuclei from those created by protons. From simulations we find that $\sigma_{p\text{-air}}^{\text{prod}}$ is overestimated depending on the percentages of helium in the data sample. Lack of knowledge of the helium fraction is the dominant source of systematic uncertainty.

We also find that the nuclei of the CNO group introduce no bias for fractions up to $\sim 50\%$, and accordingly we assign no uncertainty in the cross section due to these or heavier nuclei.

In Table I, we list the sources of systematic uncertainties. As the helium fraction is not known, we show the impact of 10, 25, and 50% of helium, respectively. In what follows we include a systematic uncertainty related to a helium fraction of 25%. In the extreme case, were the cosmic-ray composition to be 100% helium, the analysis would overestimate the proton-air cross section by 300 to 500 mb. Given the constraints from accelerator data at lower energies and typical model assumptions, this extreme scenario is not realistic.

We summarize our results by averaging the four values of the cross section obtained with the hadronic interaction models to give

$$\sigma_{p\text{-air}}^{\text{prod}} = [505 \pm 22(\text{stat})_{-36}^{+28}(\text{syst})] \text{ mb}$$

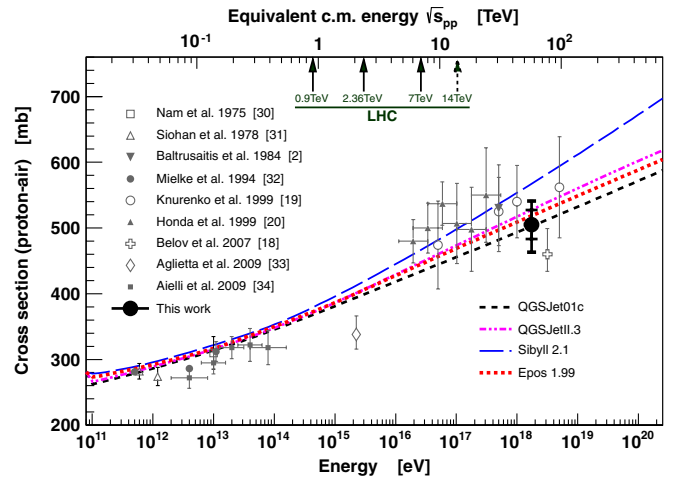


FIG. 2 (color online). Resulting $\sigma_{p\text{-air}}^{\text{prod}}$ compared to other measurements (see [18–20,30–34]) and model predictions. The inner error bars are statistical, while the outer include systematic uncertainties for a helium fraction of 25% and 10 mb for the systematic uncertainty attributed to the fraction of photons.

at a center-of-mass energy of $[57 \pm 0.3(\text{stat}) \pm 6(\text{syst})] \text{ TeV}$. In Fig. 2 we compare this result with model predictions and other measurements. The measurements at the highest energies are: HiRes [18] and Fly’s Eye [2] that are both based on X_{max} , Yakutsk Array [19] using Cherenkov observations, and Akeno [20] measuring electron and muon numbers at ground level. All these analyses assume a pure proton composition. In the context of a possible mixed-mass cosmic-ray composition, this can lead to large systematic effects. Also all these analyses are based on a single interaction model for describing air showers: Only HiRes uses a second model for systematic checks.

It is one of the prime aims of our analysis to have the smallest possible sensitivity to a nonproton component, and to perform a detailed systematic analysis on the uncertainties related to the mass composition. We also use all hadronic interaction models currently available for the estimation of model-related systematic effects. Furthermore, by using Eq. (2) we derive a cross section corresponding to a smooth interpolation from the Tevatron measurement to our analysis, with no inconsistencies as in earlier approaches.

Comparison with accelerator data.—For the purpose of making comparisons with accelerator data we calculate the inelastic and total proton-proton cross sections using the Glauber model. We use standard Glauber formalism [21], extended by a two-channel implementation of inelastic intermediate states [8] to account for diffraction dissociation [22]. The first channel corresponds to $p \rightarrow p$ scattering and has an amplitude of Γ_{pp} , while the amplitude for the other channel is $\Gamma_{pp^*} = \lambda \Gamma_{pp}$ and corresponds to the excitation of a short-lived intermediate state. The parameter λ is related to the ratio of single-diffractive cross section and elastic cross section. We use a value of $\lambda = 0.5 \pm 0.15$ that is determined from measurements of

the single-diffractive cross section, as well as from proton-carbon cross-section data at lower energies.

This Glauber calculation is model-dependent since neither the parameters nor the physical processes involved are known accurately at cosmic-ray energies. In particular, this applies to the elastic slope parameter, B_{el} (defined by $d\sigma_{el}/dt \propto \exp(-|t|B_{el})$ for very small t), the correlation of B_{el} to the cross section, and the cross section for diffractive dissociation. For the example of σ_{pp}^{inel} , the correlation of B_{el} with the cross section is shown in Fig. 3 for $\lambda = 0.5$. We have used the same four hadronic interaction models to determine the uncertainty band of the B_{el} - σ_{pp}^{inel} correlation. Recent cross-section models such as [23] fall within this band. We find that in the Glauber framework the *inelastic* cross section is less dependent on model assumptions than the *total* cross section. The result for the inelastic proton-proton cross section is

$$\sigma_{pp}^{inel} = [92 \pm 7(\text{stat})_{-11}^{+9}(\text{syst}) \pm 7(\text{Glauber})] \text{ mb},$$

and the total proton-proton cross section is

$$\sigma_{pp}^{tot} = [133 \pm 13(\text{stat})_{-20}^{+17}(\text{syst}) \pm 16(\text{Glauber})] \text{ mb}.$$

The systematic uncertainties for the inelastic and total cross sections include contributions from the elastic slope parameter, from λ , from the description of the nuclear density profile, and from cross-checking these effects using QGSJETII [9,24]. For the inelastic case, these three independent contributions are 1, 3, 5, and 4 mb, respectively. For the total cross section, they are 13, 6, 5, and 4 mb. We emphasize that the total theoretical uncertainty of converting the proton-air to a proton-proton cross section may be larger than estimated here within the Glauber model. There are other extensions of the

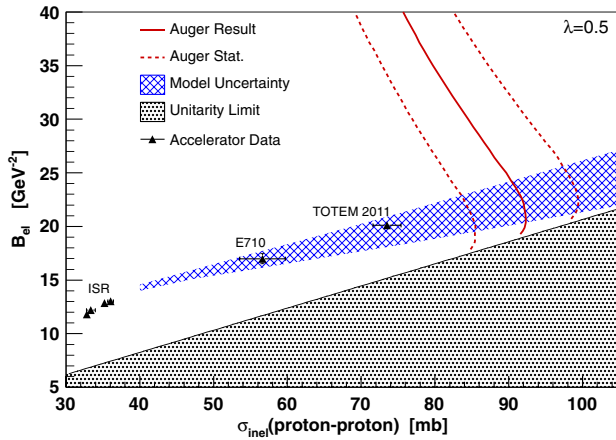


FIG. 3 (color online). Correlation of elastic slope parameter, B_{el} , and the inelastic proton-proton cross section in the Glauber framework. The solid line indicates the parameter combinations yielding the observed proton-air production cross section, and the dotted lines are the statistical uncertainties. The hatched area corresponds to the predictions by SIBYLL, QGSJET, QGSJETII, and EPOS. See also Ref. [5].

Glauber model to account for inelastic screening [8,25] or nucleon-nucleon correlations [26], and alternative approaches that include, for example, parton saturation or other effects [11,24,27,28].

In Fig. 4 we compare our inelastic cross-section result to accelerator data and to the cross sections used in the hadronic interaction models.

Summary.—We have presented the measurement of the cross section for the production of particles in proton-air collisions from data collected at the Pierre Auger Observatory. We have studied in detail the effects of assumptions on the primary cosmic-ray mass composition, hadronic interaction models, simulation settings, and the fiducial volume limits of the telescopes on the final result. By analyzing only the most deeply penetrating events, we selected a data sample enriched in protons. The results are presented assuming a maximum contamination of 25% of helium in the light cosmic-ray mass component. The lack of knowledge of the helium component is the largest source of systematic uncertainty. However, for helium fractions up to 25% the induced bias remains below 6%.

To derive a value of $\sigma_{p\text{-air}}^{\text{prod}}$ from the measured Λ_{η} , we assume a smooth extrapolation of hadronic cross sections from accelerator measurements to the energy of the analysis. This is achieved by modifying the model predictions of hadronic cross sections above energies of 10^{15} eV during the air-shower simulation process in a self-consistent approach.

We convert the proton-air production cross section into the total, and the inelastic, proton-proton cross section using a Glauber calculation that includes intermediate inelastic screening corrections. In this calculation, we use the correlation between the elastic slope parameter and the proton-proton cross sections taken from the interaction models as a constraint. We find that the inelastic proton-proton cross section depends less on the elastic slope parameter than

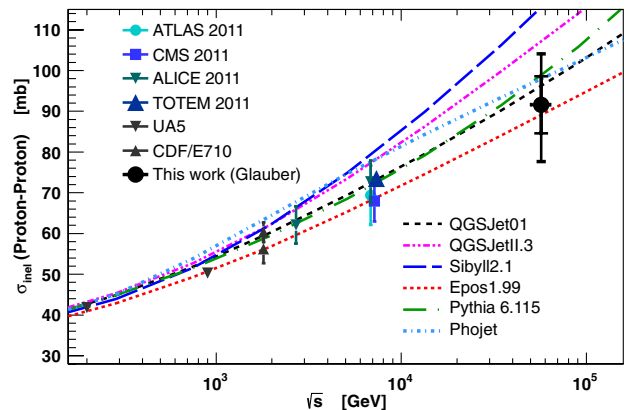


FIG. 4 (color online). Comparison of derived σ_{pp}^{inel} to model predictions and accelerator data [29]. Here we also show the cross sections of two typical high-energy models, PYTHIA6 [35] and PHOJET [36]. The inner error bars are statistical, while the outer include systematic uncertainties.

does the total proton-proton cross section, and thus the systematic uncertainty of the Glauber calculation for the inelastic result is smaller. The data agree with an extrapolation from LHC [29] energies to 57 TeV for a limited set of models.

The successful installation, commissioning, and operation of the Pierre Auger Observatory would not have been possible without the strong commitment and effort from the technical and administrative staff in Malargüe. We are very grateful to the following agencies and organizations for financial support: Comisión Nacional de Energía Atómica, Fundación Antorchas, Gobierno De La Provincia de Mendoza, Municipalidad de Malargüe, NDM Holdings and Valle Las Leñas, in gratitude for their continuing cooperation over land access, Argentina; the Australian Research Council; Conselho Nacional de Desenvolvimento Científico e Tecnológico (CNPq), Financiadora de Estudos e Projetos (FINEP), Fundação de Amparo à Pesquisa do Estado de Rio de Janeiro (FAPERJ), Fundação de Amparo à Pesquisa do Estado de São Paulo (FAPESP), Ministério de Ciência e Tecnologia (MCT), Brazil; AVCR AV0Z10100502 and AV0Z10100522, GAAV KJB100100904, MSM-T-CR LA08016, LC527, 1M06002, MEB111003, and MSM0021620859, Czech Republic; Centre de Calcul IN2P3/CNRS, Centre National de la Recherche Scientifique (CNRS), Conseil Régional Ile-de-France, Département Physique Nucléaire et Corpusculaire (PNC-IN2P3/CNRS), Département Sciences de l'Univers (SDU-INSU/CNRS), France; Bundesministerium für Bildung und Forschung (BMBF), Deutsche Forschungsgemeinschaft (DFG), Finanzministerium Baden-Württemberg, Helmholtz-Gemeinschaft Deutscher Forschungszentren (HGF), Ministerium für Wissenschaft und Forschung, Nordrhein-Westfalen, Ministerium für Wissenschaft, Forschung und Kunst, Baden-Württemberg, Germany; Istituto Nazionale di Fisica Nucleare (INFN), Ministero dell'Istruzione, dell'Università e della Ricerca (MIUR), Italy; Consejo Nacional de Ciencia y Tecnología (CONACYT), Mexico; Ministerie van Onderwijs, Cultuur en Wetenschap, Nederlandse Organisatie voor Wetenschappelijk Onderzoek (NWO), Stichting voor Fundamenteel Onderzoek der Materie (FOM), Netherlands; Ministry of Science and Higher Education, Grant Nos. N N202 200239 and N N202 207238, Poland; Fundação para a Ciência e a Tecnologia, Portugal; Ministry for Higher Education, Science, and Technology, Slovenian Research Agency, Slovenia; Comunidad de Madrid, Consejería de Educación de la Comunidad de Castilla La Mancha, FEDER funds, Ministerio de Ciencia e Innovación and Consolider-Ingenio 2010 (CPAN), Xunta de Galicia, Spain; Science and Technology Facilities Council, United Kingdom; Department of Energy, Contract Nos. DE-AC02-07CH11359, DE-FR02-04ER41300, National Science Foundation, Grant No. 0450696, the Grainger Foundation, USA; ALFA-EC/HELEN, European Union 6th Framework

Program, Grant No. MEIF-CT-2005-025057, European Union 7th Framework Program, Grant No. PIEF-GA-2008-220240, and UNESCO.

-
- [1] J. Abraham *et al.*, *Nucl. Instrum. Methods Phys. Res., Sect. A* **523**, 50 (2004).
 - [2] R. Ellsworth, T. Gaisser, T. Stanev, and G. Yodh, *Phys. Rev. D* **26**, 336 (1982); R. Baltrusaitis, G. Cassiday, J. Elbert, P. Gerhardy, S. Ko, E. Loh, Y. Mizumoto, P. Sokolsky, and D. Steck, *Phys. Rev. Lett.* **52**, 1380 (1984).
 - [3] P. Sommers, *Astropart. Phys.* **3**, 349 (1995); B. Dawson, H. Dai, P. Sommers, and S. Yoshida, *Astropart. Phys.* **5**, 239 (1996).
 - [4] P. Facal for the Pierre Auger Collaboration, *Proceedings of the 32nd International Cosmic Ray Conference, Beijing, 2011* (2011), Vol. 2, p. 105, [arXiv:1107.4804v1](#); D. Garcia-Pinto for the Pierre Auger Collaboration, *Proceedings of the 32nd International Cosmic Ray Conference, Beijing, 2011* (2011), Vol. 2, p. 87, [arXiv:1107.4804v1](#).
 - [5] R. Engel, T. Gaisser, P. Lipari, and T. Stanev, *Phys. Rev. D* **58**, 014019 (1998).
 - [6] J. Abraham *et al.*, *Phys. Rev. Lett.* **104**, 091101 (2010).
 - [7] R. Ulrich, J. Bluemer, R. Engel, F. Schuessler, and M. Unger, *New J. Phys.* **11**, 065018 (2009).
 - [8] N. Kalmykov and S. Ostapchenko, *Phys. At. Nucl.* **56**, 346 (1993).
 - [9] S. Ostapchenko, *Phys. Rev. D* **74**, 014026 (2006).
 - [10] E. Ahn, R. Engel, T. Gaisser, P. Lipari, and T. Stanev, *Phys. Rev. D* **80**, 094003 (2009).
 - [11] K. Werner, F.M. Liu, and T. Pierog, *Phys. Rev. C* **74**, 044902 (2006).
 - [12] R. Parsons, C. Bleve, S. Ostapchenko, and J. Knapp, *Astropart. Phys.* **34**, 832 (2011).
 - [13] J. Matthews, *Astropart. Phys.* **22**, 387 (2005).
 - [14] R. Ulrich, R. Engel, and M. Unger, *Phys. Rev. D* **83**, 054026 (2011).
 - [15] R. Pesce for the Pierre Auger Collaboration, *Proceedings of the 32nd International Cosmic Ray Conference, Beijing, 2011* (2011), Vol. 2, p. 214, [arXiv:1107.4809v1](#).
 - [16] A. Glushkov, I. Makarov, M. Pravdin, I. Slepstov, D. Gorbunov, G. Rubtsov, and S. Troitsky, *Phys. Rev. D* **82**, 041101 (2010).
 - [17] M. Settimo for the Pierre Auger Collaboration, *Proceedings of the 32nd International Cosmic Ray Conference, Beijing, 2011* (2011), Vol. 2, p. 55, [arXiv:1107.4804v1](#).
 - [18] K. Belov *et al.*, *Nucl. Phys. B, Proc. Suppl.* **151**, 197 (2006).
 - [19] S. Knurenko *et al.*, *Proceedings of the 26th International Cosmic Ray Conference, Salt Lake City, 1999* (1999), Vol. 1, p. 372 (unpublished).
 - [20] M. Honda, M. Nagano, S. Tonwar, K. Kasahara, T. Hara, N. Hayashida, Y. Matsubara, M. Teshima, and S. Yoshida, *Phys. Rev. Lett.* **70**, 525 (1993).
 - [21] R. Glauber, *Phys. Rev.* **100**, 242 (1955); R. Glauber and G. Matthiae, *Nucl. Phys.* **B21**, 135 (1970).

- [22] M. Good and W. Walker, *Phys. Rev.* **120**, 1857 (1960).
- [23] M. Block, *Phys. Rep.* **436**, 71 (2006).
- [24] S. Ostapchenko, *Phys. Rev. D* **81**, 114028 (2010).
- [25] V. Guzey and M. Strikman, *Phys. Lett. B* **633**, 245 (2006).
- [26] G. Baym, B. Blattel, L. L. Frankfurt, H. Heiselberg, and M. Strikman, *Phys. Rev. C* **52**, 1604 (1995).
- [27] D. R. Harrington, *Phys. Rev. C* **67**, 064904 (2003).
- [28] L. Frankfurt, G. A. Miller, and M. Strikman, *Phys. Rev. Lett.* **71**, 2859 (1993).
- [29] TOTEM Collaboration, *Europhys. Lett.* **96**, 21002 (2011); ATLAS Collaboration, *Nature Commun.* **2**, 463 (2011); CMS Collaboration, [arXiv:1205.3142v1](https://arxiv.org/abs/1205.3142v1); ALICE Collaboration, Minimum Bias and Underlying Event Working Group, CERN Report No. 17.6.2011.
- [30] R. Nam *et al.*, *Proceedings of the 14th International Cosmic Ray Conference, Munich, 1975* (1975), p. 2258 (unpublished).
- [31] F. Siohan, R. Ellsworth, A. Ito, J. MacFall, R. Streitmatter, S. Tonwar, and G. Yodh, *J. Phys. G* **4**, 1169 (1978).
- [32] H. Mielke, M. Foller, J. Engler, and J. Knapp, *J. Phys. G* **20**, 637 (1994).
- [33] M. Aglietta *et al.* (EAS-TOP Collaboration), *Phys. Rev. D* **79**, 032004 (2009).
- [34] G. Aielli *et al.* (ARGO Collaboration), *Phys. Rev. D* **80**, 092004 (2009).
- [35] G. A. Schuler and T. Sjostrand, *Phys. Rev. D* **49**, 2257 (1994).
- [36] R. Engel, *Z. Phys. C* **66**, 203 (1995); R. Engel and J. Ranft, *Phys. Rev. D* **54**, 4244 (1996).